Cell Metabolism, Volume *18*
Supplemental Information

KATP-Channel-Dependent Regulation of Catecholaminergic Neurons Controls BAT Sympathetic Nerve Activity and Energy Homeostasis

Sulay Tovar, Lars Paeger, Simon Hess, Donald A. Morgan, A. Christine Hausen, Hella S. Brönneke, Brigitte Hampel, P. Justus Ackermann, Nadine Evers, Hildegard Büning, F. Thomas Wunderlich, Kamal Rahmouni, Peter Kloppenburg, and Jens C. Brüning

Supplementary Figure 1
Tovar et al

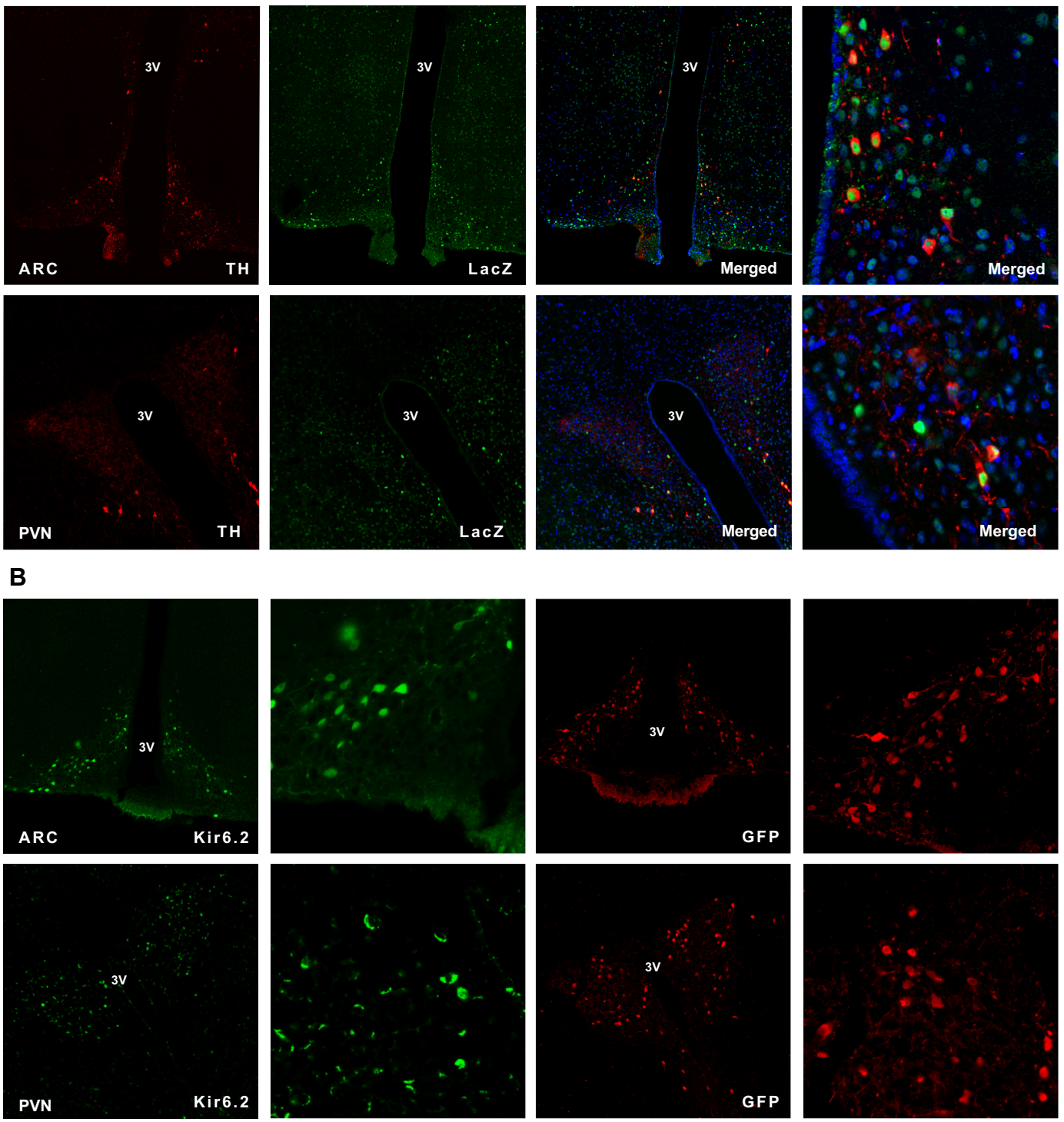

Figure S1. Endogenous TH, Kir6.2, and Cre-Dependent LacZ/GFP Expression in Different Brain Areas, Related to Figures 1A and 1B

(A) Visualization of Cre-activity in TH-Cre-LacZ reporter mice. Double immunofluorescence for endogenous TH and transgenically expressed β-galactosidase (β-gal) in different brain regions of double-heterozygous TH-Cre-LacZ reporter mice. Nuclear staining: blue (DAPI), β-galactosidase staining: green (β-gal), tyrosine hydroxylase: red (TH). Hypothalamic arcuate nucleus (ARC), paraventricular hypothalamic nucleus (PVN). Details are shown in a higher magnification.

(B) Expression of Kir6.2 in catecholaminergic neurons. Immunofluorescence detection of Kir6.2 expression and GFP in adjacent sections of double-heterozygous TH-Cre-GFP reporter mice. TH-IRES-Cre negative littermates were used as controls. green (Kir6.2); red (GFP). Hypothalamic arcuate nucleus (ARC), paraventricular hypothalamic nucleus (PVN). Details are shown in a higher magnification.

Supplementary Figure 2
Tovar et al

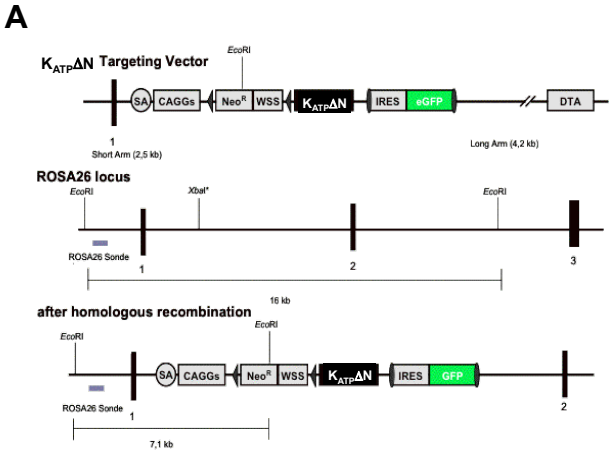

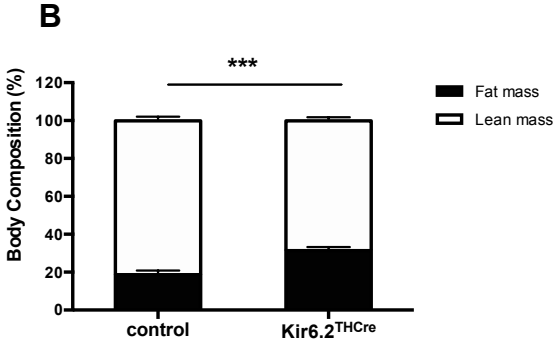

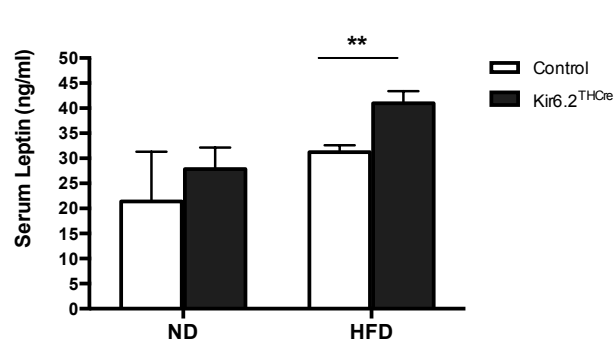

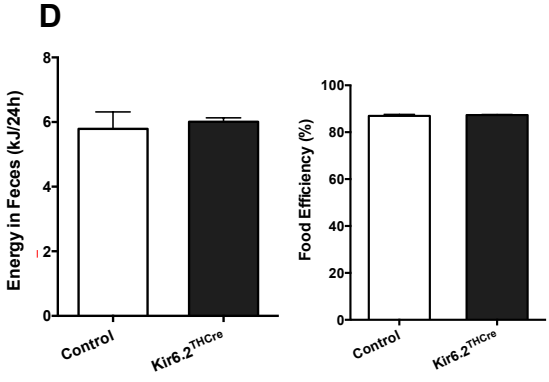

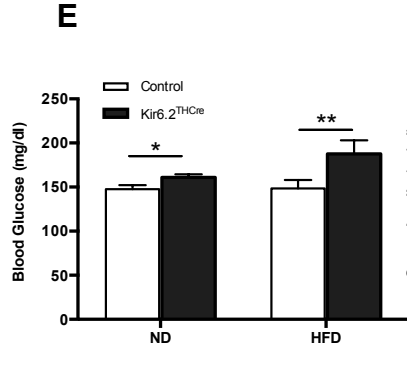

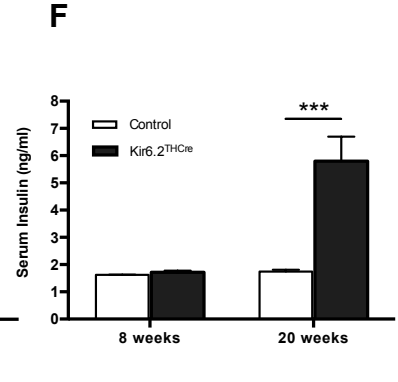

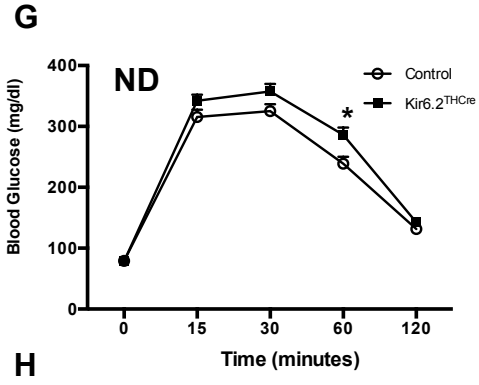

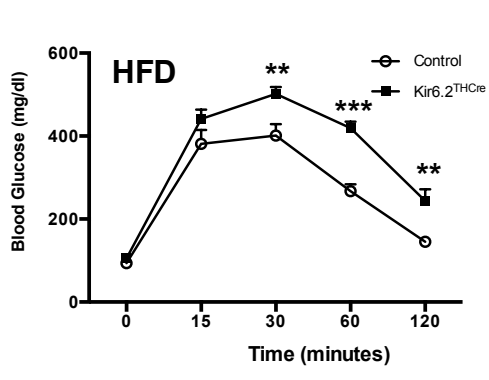

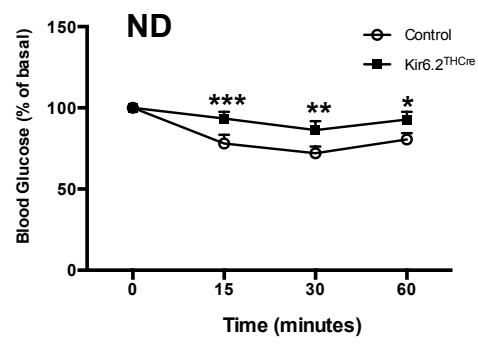

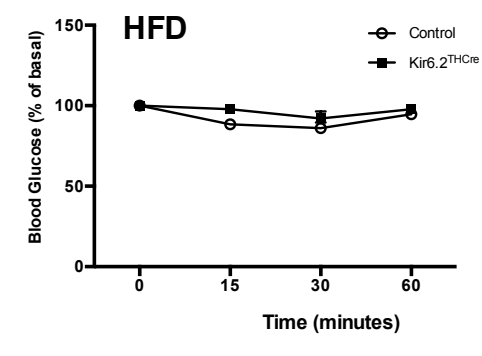

Figure S2. Generation and Physiological Characterization of Kir6.2$^{TH\text{-}Cre}$ Mice, Related to Figures 1C–1H

(A) Conditional expression of Kir6.2[K185Q,ΔN30] in mice. Schematic representation of the targeting vector ROSA26-STOP-Kir6.2[K185Q,ΔN30] introduced in the ROSA26 locus via homologous recombination in murine ES cells.

(B) Average body fat content of 20-week-old male control (n=12) and Kir6.2^{THCre}–mice (n=16) on normal chow (ND) measured by nuclear magnetic resonance.

(C) Serum leptin concentrations of 20-week-old male control and Kir6.2^{THCre}-mice on ND (control, n=10; Kir6.2^{THCre}, n=10) and on HFD (control, n=9; Kir6.2^{THCre}, n=11) as determined by ELISA.

(D) Feces energy measurements: Energy in feces (kJ/24 h) (left panel) and food efficiency (%, right panel) in control (n=8) and Kir6.2^{THCre}-mice (n=14) on HFD.

(E) Blood glucose concentrations of 20-week-old male control and Kir6.2^{THCre}-mice on ND (control, n=15; Kir6.2^{THCre}, n=20) and on HFD (control, n=14; Kir6.2^{THCre}, n=15).

(F) Serum insulin concentrations of 8 (control, n=7; Kir6.2^{THCre}, n=8) and 20-week-old (control, n=8; Kir6.2^{THCre}, n=8) male control and Kir6.2^{THCre}-mice on HFD.

(G) Glucose tolerance test of male control and Kir6.2^{THCre}-mice on ND (control, n=22; Kir6.2^{THCre}, n=24) and on HFD (control, n=12; Kir6.2^{THCre}, n=14) at the age of 10 weeks.

(H) Insulin tolerance test of male control and Kir6.2^{THCre}-mice on ND (control, n=23; Kir6.2^{THCre}, n=23) and on HFD (control, n=12; Kir6.2^{THCre}, n=14) at the age of 10 weeks.

Data is expressed as mean ±SEM. *$p<0.05$, **$p<0.01$, ***$p<0.001$ between control and Kir6.2^{THCre}-mice.

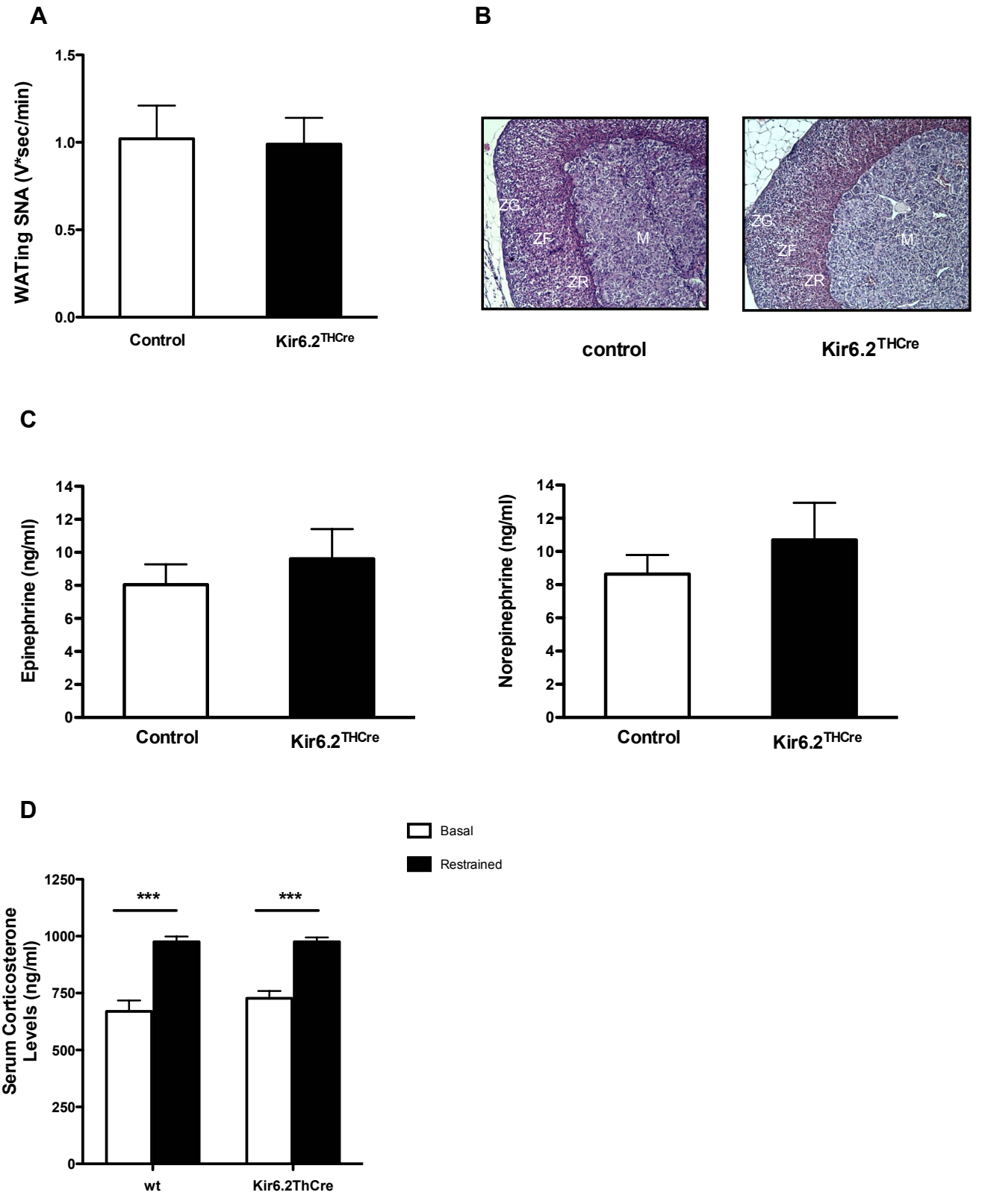
A
WATing SNA (V*sec/min)
1.5
1.0
0.5
0.0
Control
Kir6.2THCre
B
ZG
ZF
M
ZR
control
Kir6.2THCre
C
Epinephrine (ng/ml)
14
12
10
8
6
4
2
0
Control
Kir6.2THCre
Norepinephrine (ng/ml)
Control
Kir6.2THCre
D
Basal
Restrained
Serum Corticosterone Levels (ng/ml)
1250
1000
750
500
250
0
***
***
wt
Kir6.2ThCre

Figure S3. Unaltered Adrenal Gland Morphology and Function in Kir6.2$^{TH\text{-}Cre}$ Mice, Related to Figure 2

(A) Inguinal white adipose tissue (WATing) sympathetic nerve activity (SNA) recordings in 15-week-old control (n=5) and Kir6.2^{THCre}-mice (n=5) on HFD.

(B) Representative H&E stainings of adrenal glands of control mice and Kir6.2^{THCre}-mice at the age of 15 weeks (ZG: Granulose zone, ZF: Fascicular zone, ZR: Reticular zone, M: Medulla).

(C) Plasma epinephrine and norepinephrine concentrations of 15-week-old control and Kir6.2^{THCre}-mice (epinephrine: control, n=7; Kir6.2^{THCre}, n=8; norepinephrine: control, n=7; Kir6.2^{THCre}, n=7) on a HFD as determined by ELISA.

(D) Serum corticosterone levels of 20-week-old control (n=11) and Kir6.2^{THCre}-mice (n=14) on HFD as determined by ELISA.

Data is expressed as mean ±SEM. ***$p<0.001$ between control and Kir6.2^{THCre}-mice.

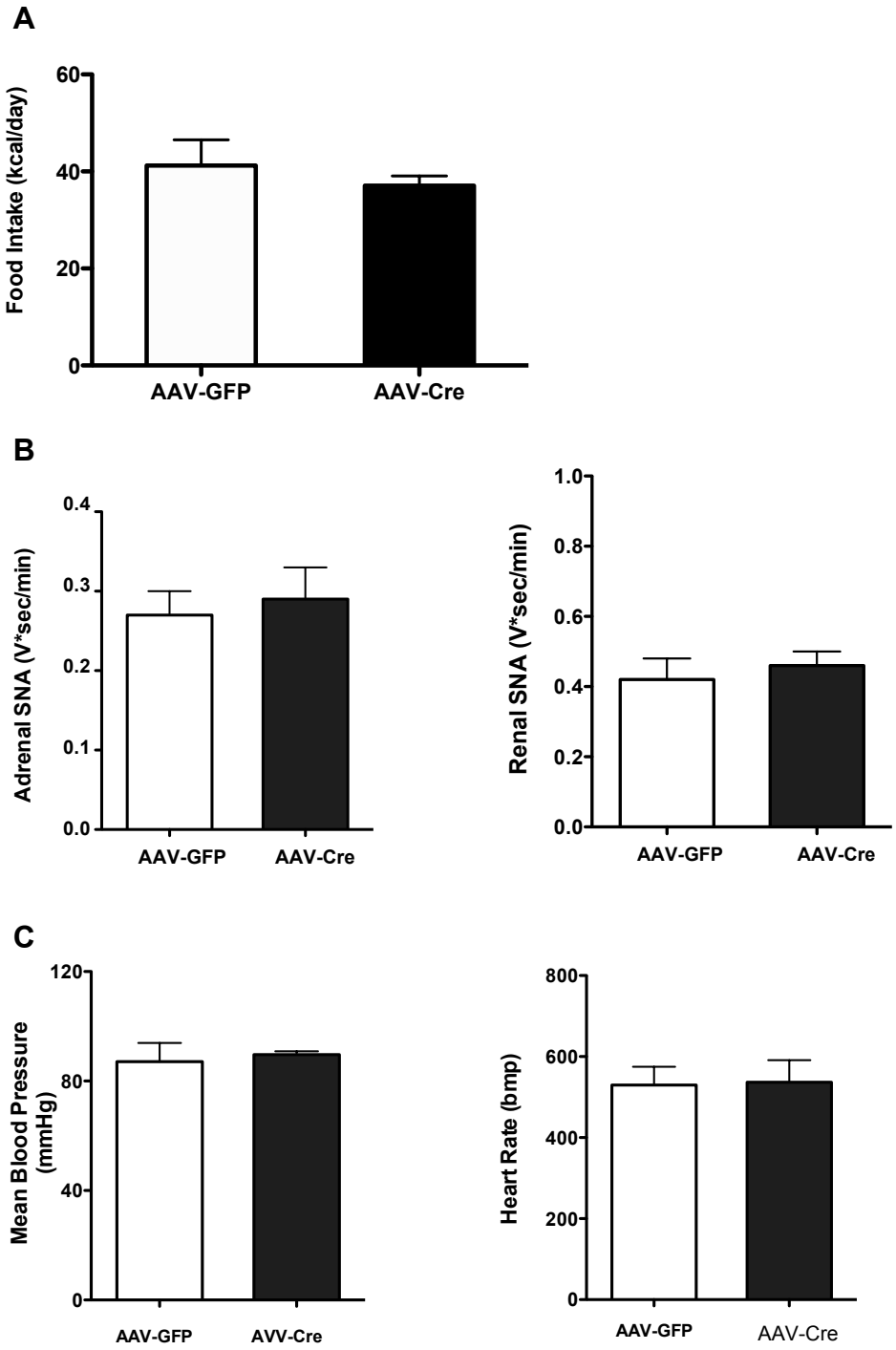
A
Food Intake (kcal/day)
60
40
20
0
AAV-GFP
AAV-Cre
B
Adrenal SNA (V*sec/min)
0.4
0.3
0.2
0.1
0.0
AAV-GFP
AAV-Cre
Renal SNA (V*sec/min)
1.0
0.8
0.6
0.4
0.2
0.0
AAV-GFP
AAV-Cre
C
Mean Blood Pressure (mmHg)
120
80
40
0
AAV-GFP
AVV-Cre
Heart Rate (bmp)
800
600
400
200
0
AAV-GFP
AAV-Cre

Figure S4. AAV-Mediated, LC-Specific Expression of the Mutant Form of Kir6.2, Related to Figure 4

(A) Average daily food intake of control (AAV-GFP, n=6) and AAV-Cre mice (n=9) on HFD measured 7 weeks after AAV vector-injection.

(B) Adrenal and renal sympathetic nerve activity (SNA) recordings of male control (AAV-GFP, n=8) and AAV-Cre mice (n=7) on HFD measured 7 weeks after AAV vector-injection.

(C) Blood pressure and heart rate measurements in fully awake and unrestrained male control (AAV-GFP, n=4) and AAV-Cre mice (n=3) on HFD measured 7 weeks after AAV vector-injection.

Data is expressed as mean ±SEM.

Supplemental Experimental Procedures

Animal Care

All animal care was within University of Cologne institutional animal care committee guidelines. All animal procedures were conducted in compliance with protocols approved by local government authorities (*Bezirksregierung Köln*, Cologne, Germany) and were in accordance with National Institutes of Health guidelines. Mice were housed in groups of 3-5 at 22°C–24°C with a 12 hr light/12 hr dark cycle. Animals were fed either a normal chow (ND; Teklad Global Rodent no. T.2018.R12; Harlan) containing 53.5% carbohydrate, 18.5% protein, and 5.5% fat (12% of calories from fat) or a high-fat diet (HFD; no. C1057, Altromin) containing 32.7% carbohydrate, 20% protein, and 35.5% fat (55.2% of calories from fat). Animals were given ad libitum access to water at all times, and food was only withdrawn if required for an experiment. Body weight was measured once per week.

Generation of Kir6.2$^{TH\text{-}Cre}$ Mice

Th-IRES-Cre mice (Lindeberg et al., 2004) were mated with Rosa26$^{Kir6.2}$[K185Q,ΔN30] mice (Remedi et al., 2009) and breeding colonies were maintained by mating homozygous ROSA26$^{Kir6.2}$ mice with TH-IRES-Cre mice to obtain Kir6.2^{THCre} mice and the respective controls Kir6.2^{THCre-}. ROSA26$^{Kir6.2}$ mice had been generated in V6.5 ES cells and backcrossed 10 times to C57/BL6 mice to obtain a pure C57BL/6 background. Mice were genotyped by PCR using genomic DNA isolated from tail tips. TH-IRES-Cre primers: TH-5': 5'-caccctgacccaagcact-3'; TH-3': 5'-ctttccttcctttattgagat-3'; Cre-UD: 5'-gatacctggcctggtctg-3'; CAGS primers: CAGS forw: 5'-aaagtcgctctgagttgttatc-3'; CAGS

rev-wt: 5'-gatatgaagtactgggctctt-3'; CAGS rev: 5'-tgtcgcaaattaactgtgaatc-3'.

Viral Vector Production and Purification

Recombinant AAV serotype 2 vector production (AAV) was carried out by calcium phosphate transient triple-transfection of the vector plasmid pSUBCre (for AAV-Cre), or pSUB201-GFP (for AAV-GFP), the pRC AAV2 helper plasmid and pXX680 adenovirus helper plasmid into human embryonic kidney 293 (HEK293) cells. pSubCre contained the phosphoglycerate kinase promoter driven Cre cassette that was amplified from pgkCrebPA using primers 5Ascpgk (ggc-gcg-ccg-agg-tcg-acg-gta-tcg-ata-agc-tt) and 3NotCre (gcg-gcc-gct-aat-cgc-cat-ctt-cca-gca-g), and subsequently cloned into pSub201GFP using restriction endonucleases *AscI* and *NotI*. HEK293 cells were harvested after 2 days post transfection and subjected to Benzonase treatment after lysis. AAV-cre and AAV-GFP particles were concentrated and purified using a discontinuous iodixanol gradient followed by affinity chromatography using a HiTrapHeparin column (GE Healthcare). Genomic titers were determined by quantitative real-time PCR.

In Vivo AAV Injections

Homozygous Rosa26$^{Kir6.2}$ mice (8 weeks of age, exposed to HFD from 3 weeks of age on) were anesthetized and positioned in a Stoelting stereotaxic frame. The skull was exposed, bregma was identified, and two small holes were manually drilled for bilateral injection into the locus coeruleus (-5.45 antero-posterior, -/+1.28 mediolateral and -3.65 dorso-ventral). 1 μl (1*10^8 genomic particles per μl) of AAV-GFP or (3.5*10^8 genomic particles per μl) AAV-Cre was injected in each side using a 1 μl Hamilton syringe with 28-gauge tip. After each injection the needle was maintained in position for 15 min to

prevent reflux. Thereafter, body weight was measured daily for 4 weeks following stereotactic AAV vector-injection. Brains were fixed and frozen for immunohistochemistry of GFP to verify correct injection sites.

Glucose and Insulin Tolerance Tests

Glucose and insulin tolerance tests were performed as previously described (Bruning et al., 1997). Animals were intraperitoneally injected with 2g/kg body weight of glucose (20% glucose; Delta Select) or 0.75 U/kg body weight of human regular insulin (Sanofi Aventis), respectively. Blood glucose levels were determined immediately before and 15, 30, 60 after the injection, with an additional value determined after 120 minutes for the glucose tolerance test using a hand-held blood glucose meter (GlucoMen Glycó, A. Menarini Diagnostics Deutschland, Berlin, Germany).

Body Weight and Food Intake

Body weight was measured once a week. Food intake was measured over 10 days in a regular cage using special food hoppers, which were weighed twice a week and daily food intake was calculated as the average kcal intake of chow within the time stated.

Indirect Calorimetry

Metabolic rate measurements were performed in an open circuit calorimetry system (PhenoMaster, TSE Systems GmbH, Bad Homburg, Germany). Mice were placed in regular type II cages with sealed lids of the PhenoMaster system and were allowed to acclimatize in the chambers for at least 24 hr. Food and water were provided *ad libitum*

in the appropriate devices. Presented data are average values obtained in these recordings (at least 48 hours). Energy expenditure was corrected for lean body mass.

Fecal Energy Content

Fecal samples were collected over 24h during 2 days from individual mice at 20 weeks of age and used for bomb calorimetry and SCFA analysis. For bomb calorimetry analysis, the samples were weighed and oven-dried at 60°C for 48h. After drying, food and feces samples were homogenized, squeezed to a pill and placed inside a decomposition vessel (bomb) and combusted with O_2 under high pressure. The caloric value was calculated from the heat released during the combustion process. The energy content of the feces was assessed with a Parr 6300 calorimeter using an 1109 semi-micro bomb (Parr Instruments & Co., Moline, Illinois, USA). These experiments were performed by Sanofi-Aventis.

Cold Exposure

Mice were fasted for 1 hour before they were placed in a room at 4°C. We measured the core body temperature at the indicated times before and during cold exposure using a rectal probe attached to a digital thermometer (Harvard Apparatus, Holliston, MA, USA).

Analytical Procedures

Blood glucose values were determined from whole venous blood using an automatic glucose monitor (*GlucoMen Glycó*, A. Menarini Diagnostics, Deutschland, Berlin, Germany). Serum insulin and leptin levels and epinephrine and norepinephrine plasma levels were measured by ELISA using mouse standards according to manufacturer

guidelines (Mouse Leptin ELISA, Crystal Chem Inc. Downers Grove, IL, USA; Insulin Mouse Ultrasensitive ELISA, Adrenalin and Noradrenalin Research ELISA, DRG Instruments GmbH, Marburg, Germany). For corticosterone measurements, plasma samples of control and Kir6.2^{THCre}-mice under unstressed and restrained conditions were analyzed with a Corticosterone ELISA (Enzo®) according to manufacturer guidelines.

Immunohistochemistry

TH-IRES-Cre mice were mated with a ROSA-Arte1 (LacZ) reporter mouse strain (Seibler et al., 2003) for Cre-dependent expression of a *β-galactosidase* gene (Th-IRES-Cre-LacZ). Additionally, a second reporter mouse strain was used, which expresses enhanced green fluorescent protein (GFP) upon Cre-mediated recombination (Th-IRES-Cre-GFP) (Novak et al., 2000).

Double heterozygous mice were anesthetized and transcardially perfused with physiologic saline solution followed by 4% paraformaldehyde (PFA) in 0.1 M phosphate-buffered saline (PBS; pH 7.4). Brains were removed, postfixed in 4% PFA at 4°C, transferred to 20% sucrose for 6 hr, and frozen in tissue freezing medium. Then, 25 µm thick free-floating coronal sections were cut through the arcuate nucleus, paraventricular nucleus, ventrotegmental area, substantia nigra, locus coeruleus, and rostroventrolateral medulla using a freezing microtome (Leica). The sections were collected in PBS (pH 7.4) and stored in antifreeze solution (50% PBS, 15% ethyl glycol, 35% glycerol) at −20°C until further use.

For immunostaining of GFP and/or Kir6.2 in TH-IRES-Cre-GFP mice *or* ROSA26$^{Kir6.2}$-mice, which were injected with AAV-GFP or AAV-Cre, 25-µm-thick free-floating

coronal sections were dissected using a freezing microtome (Leica) and stored in antifreeze solution (50% PBS, 15% ethyl glycol, 35% glycerol) at −20°C. Free-floating tissue sections were extensively washed to remove cryoprotectant, incubated for 20 minutes at room temperature in 0.3% glycine in PBS for 10 minutes and 0.03% SDS in PBS for 10 minutes, including PBS washes during the steps. After washing, sections were blocked for 1h (3% normal goat serum in PBS, 0.4% Triton X-100, 0.2% sodium-azide) followed by incubation of primary antibody anti-EGFP (1:10000 diluted in blocking solution; #A6455; Invitrogen/molecular), rabbit anti-Th (ab112; Abcam) diluted 1:1000 in SignalStain® Antibody Diluent #8112 (Cell Signaling) or goat anti-kir6.2 (sc11226; Santa Cruz) diluted 1:100 in SignalStain® Antibody Diluent #8112 (Cell Signaling) for 48 hours at 4°C Sections were extensively washed in PBS, incubated in darkness for 2 hours at room temperature in donkey anti-rabbit serum (Jackson ImmunoResearch Laboratories Inc) for GFP-detection, in goat anti-rabbit Alexa A11012 for Th-detection and in donkey anti-goat Alexa 488 (invitrogen) for Kir6.2-staining. Sections were mounted onto gelatine-coated slides, dried, and coverslipped using mounting media (ProLong Gold; Invitrogen).

For double immunofluorescence in TH-IRES-Cre-LacZ reporter mice, sections were treated as free-floating coronal sections. After washing and blocking, sections were incubated with rabbit anti-Th (ab112; Abcam) and with chicken anti-LacZ (ab 9361;Abcam) both diluted 1:1000 in SignalStain® Antibody Diluent #8112 (Cell Signaling); overnight at room temperature. Sections were extensively washed in PBS, incubated in darkness for 2 hours at room temperature in goat anti-chicken FITC (1:500; Jackson ImmunoResearch Laboratories Inc) and goat anti-rabbit-Alexa (1:500; A11012).

Sections were mounted onto gelatine-coated slides, dried, and coverslipped using mounting media (ProLong Gold; Invitrogen). Fluorescence signals were detected under a Meta Zeiss 510 confocal microscope and for images processing Zeiss LSM Image software was used. For endogenous TH-/Kir6.2 and LacZ/GFP expression studies TH-IRES-Cre negative littermates were used as controls.

For immunostaining of cells in the LC and co-labeling with biocytin, standard protocols have been used (rabbit anti-dopamine- β -hydroxylase [abcam, ab46868, 1:250]; goat anti-rabbit-Alexa488 [abcam, ab150077, 1:100]; streptavidin-Alexa633 [Invitrogen, s21375, 1:400).

Electrophysiology

Animals and Brain Slice Preparation

Electrophysiological experiments were performed on brain slices from 70- to 105-day old female and male mice. The animals were anesthetized with halothane (B4388; Sigma-Aldrich, Taufkirchen, Germany) and subsequently decapitated. The brain was rapidly removed and a block of tissue containing the brainstem was immediately cut out. Coronal slices (250 - 300µm) containing the *locus coeruleus* (LC) were cut with a vibration microtome (HM-650 V; Thermo Scientific, Walldorf, Germany) under cold (4 °C), carbonated (95% O_2 and 5% CO_2), glycerol-based modified artificial cerebrospinal fluid (GaCSF; (Ye et al., 2006)) to enhance the viability of neurons. GaCSF contained (in mM): 250 Glycerol, 2.5 KCl, 2 $MgCl_2$, 2 $CaCl_2$, 1.2 NaH_2PO_4, 10 HEPES, 21 $NaHCO_3$, 5 Glucose adjusted to pH 7.2 (with NaOH) resulting in an osmolarity of ~310 mOsm. Brain slices were transferred into carbogenated artificial cerebrospinal fluid (aCSF). First, they

were kept for 20 min in a 35 °C 'recovery bath' and then stored at room temperature (24 °C) for at least 30 min prior to recording. aCSF contained (in mM): 125 NaCl, 2.5 KCl, 2 $MgCl_2$, 2 $CaCl_2$, 1.2 NaH_2PO_4, 21 $NaHCO_3$, 10 HEPES, and 5 Glucose adjusted to pH 7.2 (with NaOH) resulting in an osmolarity of ~310 mOsm.

Perforated Patch Recordings

Slices were transferred to a recording chamber (~3 ml volume) and continuously superfused with carbogenated aCSF at a flow rate of ~2 $ml \cdot min^{-1}$. Neurons in LC were visualized with a fixed-stage upright microscope (BX51WI; Olympus, Hamburg, Germany), using a 60× water immersion objective (LUMplan FI/IR; 60×; 0.9 numerical aperture; 2 mm working distance; Olympus) with infrared-differential interference contrast and fluorescence optics. In the LC TH positive cells were identified by their GFP fluorescence (Chroma 41001 filter set; EX: HQ480/40x, BS: Q505LP, EM: HQ535/50m, Chroma, Rockingham, VT, USA), or by their position at the ventrolateral border of the fourth ventricle and by norepinephrine (100 μM) induced hyperpolarization (Finta et al., 1993). The effect of norepinephrine was tested at the end of the experiment after the tolbutamide application (see glucose sensing experiments).

Current-clamp recordings in the perforated patch configuration were performed with an EPC10 patch-clamp amplifier (HEKA, Lambrecht, Germany) controlled by the PatchMaster software (version 2.32; HEKA) running under Windows. Data were sampled at intervals of 100 μs (10 kHz) and low-pass filtered at 2 kHz with a four-pole Bessel filter. The liquid junction potential between intracellular and extracellular solution was compensated (14.6 mV for normal aCSF; calculated with Patcher's Power Tools plug-in

downloaded from http://www.mpibpc.gwdg.de/abteilungen/140/software/index.html for Igor Pro 6 [Wavemetrics, Lake Oswego, OR, USA]).

Perforated patch recordings were performed using protocols modified from Horn and Marty (Horn and Marty, 1988) and Akaike and Harata (Akaike and Harata, 1994). Electrodes with tip resistances between 3 and 5 MOhm were fashioned from borosilicate glass (0.86 mm inner diameter; 1.5 mm outer diameter; GB150-8P; Science Products) with a vertical pipette puller (PP-830; Narishige, London, UK). Perforated patch recordings were performed with ATP and GTP free pipette solution containing (in mM): 128 K-gluconate, 10 KCl, 10 HEPES, 0.1 EGTA, 2 $MgCl_2$ and adjusted to pH 7.3 (with KOH) resulting in an osmolarity of ~300 mOsm. ATP and GTP were omitted from the intracellular solution to prevent uncontrolled permeabilization of the cell membrane (Lindau and Fernandez, 1986). The patch pipette was tip filled with internal solution and back filled with tetraethylrhodamine-dextran (D3308, Invitrogen, Eugene, OR, USA) and amphotericin B-containing internal solution (100-250 $\mu g \cdot ml^{-1}$; A4888; Sigma) to achieve perforated patch recordings. Amphotericin B was dissolved in dimethyl sulfoxide (final concentration: 0.2 - 0.5%; DMSO; D8418, Sigma) as described in (Rae et al., 1991) and was added to the modified pipette solution shortly before use. The used DMSO concentration had no obvious effect on the investigated neurons. Experiments were carried out at ~31°C using an inline solution heater (SH27B; Warner Instruments, Hamden, CT, USA) operated by a temperature controller (TC-324B; Warner Instruments). During the perforation process access resistance (R_a) was constantly monitored and experiments were started after R_a and the action potential (AP) amplitude were stable (~15 – 30 min). A change to the whole-cell configuration was indicated by

diffusion of tetraethylrhodamine-dextran into the neuron and since we use an ATP-free pipette solution, a change to the whole-cell configuration was obvious by a spontaneous hyperpolarization of the neuron (due to K_{ATP}–channel activation). Such experiments were rejected.

Drugs. Drugs were bath-applied at a flow rate of ~2 ml·min^{-1}. The K_{ATP} channel blocker tolbutamide (200 μM; T0891, Sigma) was dissolved in DMSO and added to the normal aCSF with a final DMSO concentration of 0.25%. The DMSO concentration had no obvious effect on the investigated neurons.

Glucose-Sensing Experiments

To study glucose sensing we used modified protocols from Parton et al. (Parton et al., 2007) and varied bath glucose concentrations between 3 and 8 mM. in normal aCSF or aCSF containing 10^{-4} M PTX, 5 x 10^{-5} M D-AP5, and 10^{-5} M CNQX to block synaptic input. Since we found no difference in relative effects of external glucose changes by blocking synaptic input, the recorded cells were pooled for both saline. At the end of each experiment tolbutamide (200 μM) was applied to probe for K_{ATP} channels. We found that the basic firing properties of TH positive LC neurons and their sensitivity to glucose were not homogenous. Therefore we used the '3 times standard deviation' criterion (Dhillon et al., 2006) and considered a neuron glucose responsive when the change in firing frequency between different glucose concentrations was 3 times larger than the standard deviation. The neurons were exposed to each glucose concentration for at least 10-15 min. For each neuron, the firing rate averaged from 30s intervals was taken as one data point. To determine the mean firing rate and standard deviation 10 data points at stable firing rates were averaged. The means for glucose responses were calculated from

periods of peak hyperpolarizations or depolarizations, respectively

Data Analysis

Data analysis was performed with Igor Pro 6 (Wavemetrics) and Graphpad Prism (version 5.0b; Graphpad Software Inc., La Jolla, CA, USA). Numerical values are given as mean ± standard error. To determine differences in means, ANOVA was performed*; post hoc* pairwise comparisons were performed using *t* tests with the Newman-Keuls method for *p* value adjustment. A significance level of 0.05 was accepted for all tests. *$p \leq 0.05$; **$p \leq 0.01$;***$p \leq 0.001$ *versus* controls.

Direct Recording of BAT, WAT, Adrenal, and Renal Sympathetic Nerve Activity

Direct multifiber recording was used to compare BAT, WAT, adrenal and renal sympathetic nerve activity (SNA) between wild-type and Kir6.2^{THCre}-mice and Rosa26$^{Kir6.2}$ mice injected with AAV-Cre or AAV-GFP at baseline and in response to intracerebroventricular (icv) injection of glucose. For icv injection, mice underwent surgery one week prior to SNA recordings to implant icv cannulae as described previously (Rahmouni et al., 2003). Multi-fiber recording of SNA was obtained from the nerve subserving BAT in anesthetized mice (ketamine (91mg/kg) and xylazine (9.1mg/kg), ip). Using a dissecting microscope a nerve fiber innervating interscapular BAT was identified, placed on the bipolar platinum-iridium electrode. Each electrode was attached to a high-impedance probe (HIP-511, *Grass Instruments;* West Warwick, RI USA) and the nerve signal was amplified 10^5 times with a Grass P5 AC pre-amplifier. After amplification, the nerve signal was filtered at a 100- and 1000-Hz cutoff with a nerve traffic analysis system (Model 706C, *University of Iowa Bioengineering*, Iowa, USA). The nerve signal was then routed to an oscilloscope (model 54501A, *Hewlett-*

Packard, Iowa, USA) for monitoring the quality of the SNA recording and to a resetting voltage integrator (model B600c, *University of Iowa Bioengineering*, *Iowa, USA*). BAT SNA measurements were made during 30 minutes to compare baseline activity. To test the effect of icv glucose on BAT SNA, measurements were taken every 15 minutes over 4 hours following icv injection of vehicle (2 ml) or glucose (100 nM). To ensure that electrical noise was excluded in the assessment of BAT sympathetic traffic, each recording was corrected for post-mortem (with a lethal dose of ketamine/xylazine) background BAT sympathetic activity.

Heart Rate and Blood Pressure Measurements

Anesthesia was induced using intraperitoneal ketamine (91mg/kg) and xylazine (9.1mg/kg). Under aseptic surgery, the left carotid artery was dissected free from nearby tissue and cannulated using micro-renathane tubing (MRE-40) filled with sterile saline. The arterial catheter was tunneled behind the right forelimb where it was exited out of the nape of the neck. A 6-0 vicryl suture was used to secure the catheter to the muscle layer under the chin and to close the incision in the neck region. The cannula was filled with heparin solution (1000 U/ml, 0.1ml) and then plugged with a 22-gauge stainless steel pin. The mouse was allowed 20-24 hours to fully recover from the effects of the surgery.

The following day, the arterial cannula was briefly unplugged and the excess heparin solution was allowed to seep out until arterial blood was seen. The cannula was then quickly attached to an extension leading to a pressure transducer (BP-100, ADInstruments, Milford MA, USA). The cannula was checked for patency and when necessary flushed with sterile saline. Blood pressure and heart rate were recorded using a

two-channel tranducer amplifier (ETH-200, CB Sciences) connected to a MacLab/8s (ADInstruments, Miford, MA, USA) and a Power Macintosh G3 computer. The recording session was done while the mouse was fully awake and unrestricted in its home cage. The room was darkened and external noise and movement were restricted to minimize distractions that might excite the mouse. Each recoding session lasted 2-3 hours from which a final 10-minute segment of stable blood pressure and heart rate recordings were used for measurements.

Analysis of Gene Expression

mRNA levels in WAT and BAT were determined using the EuroScript Reverse Transcriptase (Eurogentec) and TaqMan® Assay on Demand kits (Applied Biosystems) according to the manufacturer's intructions. Probes: UCP-1 (Uncoupling Protein 1; Mm00494069), PGC1α (Peroxisome Proliferative Activated Receptor Gamma Coactivator 1-α; Mm00447183), PPARγ (Peroxisome Proliferator Activated Receptor Gamma; Mm00440945), CIDEA (Cell Death-Inducing DNA Fragmentation Factor, Alpha Subunit-Like Effector A; Mm00432554), Adrb-3 (Adrenergic Receptor, Beta 3; Mm00442669). Relative expression was determined using a comparative method (2^{-ddCt}). Assays were linear over four orders of magnitude.

Western Blotting

Brown adipose tissue was dissected and homogenized in lysis buffer using a Polytron homogenizer (IKA Werke) as previously described (Jordan et al., 2011). Western Blot analyses were carried out according to standard protocols with antibodies raised against

UCP-1 (sc-6528, Santa Cruz Biotechnology, Inc) and α-tubulin (#T6074, Sigma) as loading control. Protein levels were normalized to α-tubulin and quantified using Image-j.

Body Composition

Body fat content was measured in vivo by nuclear magnetic resonance using a minispec mq 7.5 (Bruker Optik GmbH, Ettlingen, Germany) at the age of 20 weeks.

Histomorphology

Dissected WAT, BAT and adrenal gland samples were incubated in fixation solution containing 4% PFA at 4°C overnight and embedded in paraffin according to a standard protocol (Plum et al., 2006). Sections (7µm) were mounted onto gelatin-coated slides and stained with hematoxylin and eosin (H&E; Sigma) after deparaffinization as described previously (Plum et al., 2006). Determination of mean adipocyte size was carried out in H&E-stained tissues using AxioVision 4.2 software (Carl Zeiss Microimaging).

Statistical Methods

Data sets were analyzed for statistical significance using a two-tailed unpaired Student´s T-test unless stated otherwise. All *p* values below 0.05 were considered significant. All displayed values are means ±SEM. *p≤0.05; **p≤0.01;***p≤0.001 versus controls. Energy expenditure was analyzed using an applied general linear model (GLM) and analysis of covariance (ANCOVA; R-software, http://www.r-project.org).

Supplemental References

Akaike, N., and Harata, N. (1994). Nystatin perforated patch recording and its applications to analyses of intracellular mechanisms. Jpn J Physiol 44, 433-473.

Bruning, J.C., Winnay, J., Bonner-Weir, S., Taylor, S.I., Accili, D., and Kahn, C.R. (1997). Development of a novel polygenic model of NIDDM in mice heterozygous for IR and IRS-1 null alleles. Cell 88, 561-572.

Dhillon, H., Zigman, J.M., Ye, C., Lee, C.E., McGovern, R.A., Tang, V., Kenny, C.D., Christiansen, L.M., White, R.D., Edelstein, E.A., Coppari, R., Balthasar, N., Cowley, M.A., Chua, S., Jr., Elmquist, J.K., and Lowell, B.B. (2006). Leptin directly activates SF1 neurons in the VMH, and this action by leptin is required for normal body-weight homeostasis. Neuron 49, 191-203.

Finta, E.P., Harms, L., Sevcik, J., Fischer, H.D., and Illes, P. (1993). Effects of potassium channel openers and their antagonists on rat locus coeruleus neurones. Br J Pharmacol 109, 308-315.

Horn, R., and Marty, A. (1988). Muscarinic activation of ionic currents measured by a new whole-cell recording method. J Gen Physiol 92, 145-159.

Jordan, S.D., Kruger, M., Willmes, D.M., Redemann, N., Wunderlich, F.T., Bronneke, H.S., Merkwirth, C., Kashkar, H., Olkkonen, V.M., Bottger, T., Braun, T., Seibler, J., and Bruning, J.C. (2011). Obesity-induced overexpression of miRNA-143 inhibits insulin-stimulated AKT activation and impairs glucose metabolism. Nat Cell Biol 13, 434-446.

Lindau, M., and Fernandez, J.M. (1986). IgE-mediated degranulation of mast cells does not require opening of ion channels. Nature 319, 150-153.

Lindeberg, J., Usoskin, D., Bengtsson, H., Gustafsson, A., Kylberg, A., Soderstrom, S., and Ebendal, T. (2004). Transgenic expression of Cre recombinase from the tyrosine hydroxylase locus. Genesis 40, 67-73.

Novak, A., Guo, C., Yang, W., Nagy, A., and Lobe, C.G. (2000). Z/EG, a double reporter mouse line that expresses enhanced green fluorescent protein upon Cre-mediated excision. Genesis 28, 147-155.

Parton, L.E., Ye, C.P., Coppari, R., Enriori, P.J., Choi, B., Zhang, C.Y., Xu, C., Vianna, C.R., Balthasar, N., Lee, C.E., Elmquist, J.K., Cowley, M.A., and Lowell, B.B. (2007). Glucose sensing by POMC neurons regulates glucose homeostasis and is impaired in obesity. Nature 449, 228-232.

Plum, L., Ma, X., Hampel, B., Balthasar, N., Coppari, R., Munzberg, H., Shanabrough, M., Burdakov, D., Rother, E., Janoschek, R., Alber, J., Belgardt, B.F., Koch, L., Seibler, J., Schwenk, F., Fekete, C., Suzuki, A., Mak, T.W., Krone, W., Horvath, T.L., Ashcroft, F.M., and Bruning, J.C. (2006). Enhanced PIP3 signaling in POMC neurons causes KATP channel activation and leads to diet-sensitive obesity. J Clin Invest 116, 1886-1901.

Rae, J., Cooper, K., Gates, P., and Watsky, M. (1991). Low access resistance perforated patch recordings using amphotericin B. J Neurosci Methods 37, 15-26.

Rahmouni, K., Haynes, W.G., Morgan, D.A., and Mark, A.L. (2003). Role of melanocortin-4 receptors in mediating renal sympathoactivation to leptin and insulin. J Neurosci 23, 5998-6004.

Remedi, M.S., Kurata, H.T., Scott, A., Wunderlich, F.T., Rother, E., Kleinridders, A., Tong, A., Bruning, J.C., Koster, J.C., and Nichols, C.G. (2009). Secondary consequences of beta cell inexcitability: identification and prevention in a murine model of K(ATP)-induced neonatal diabetes mellitus. Cell Metab 9, 140-151.

Seibler, J., Zevnik, B., Kuter-Luks, B., Andreas, S., Kern, H., Hennek, T., Rode, A., Heimann, C., Faust, N., Kauselmann, G., Schoor, M., Jaenisch, R., Rajewsky, K., Kuhn, R., and Schwenk, F. (2003). Rapid generation of inducible mouse mutants. Nucleic Acids Res 31, e12.

Ye, J.H., Zhang, J., Xiao, C., and Kong, J.Q. (2006). Patch-clamp studies in the CNS illustrate a simple new method for obtaining viable neurons in rat brain slices: glycerol replacement of NaCl protects CNS neurons. J Neurosci Methods 158, 251-259.